Proceedings of the Twenty-seventh (2017) International Ocean and Polar Engineering Conference **www.isope.org**
San Francisco, CA, USA, June 25-30, 2017

ISBN 978-1-880653-97-5; ISSN 1098-6189

Numerical Modeling for the Response of Bucket Foundation under Long-term Cyclic Loading

Jeong-Seon Park[1], Duhee Park[1], Hansup Kim[1], Jin-Kwon Yoo[1], Hwa-Sup Jang[2], Se-Woong Yoon[2]

[1]Department of Civil and Environmental Engineering, Hanyang University, Seoul, Korea
[2]Research center, Korea Register of Shipping, Busan, Korea

ABSTRACT

Estimation of accumulated lateral displacement and settlement are critical in design of wind turbine foundation. However, there have been few studies exploring the response of bucket foundation to long-term cyclic loading. We perform a series of three-dimensional finite element analyses of bucket foundations installed in sands and clays. An empirical formulation which captures the stiffness degradation observed in cyclic triaxial and simple shear tests is implemented into the finite element analysis in the form of a user subroutine. It is shown that the cyclically accumulated rotation of the bucket foundation increases with the number of cycles and cyclic amplitude. In particular, the magnitude of the moment and the position of the horizontal load are shown to significantly influence the cyclic response. Extensive numerical simulations are required to develop design charts for predicting the accumulated deformation of bucket foundation under long-term cyclic loading.

KEY WORDS: Cyclic loading, Bucket foundation, Finite element analysis, Long-term behavior

INTRODUCTION

Offshore wind energy has been widely developed as an alternative source of energy in the last few decades. Various types of bottom-fixed offshore wind turbines have been designed and constructed. The monopile foundation is the most common type, although bucket foundations have also been used (Zhu et al., 2013). The bucket foundation, which is typically installed using pressure difference between inside and outside of structure, has the advantage of simple and economic installation. A large body of literature on bearing capacity of bucket foundation has been published. Model tests, field tests, and numerical simulations have been performed to determine the bearing capacities of bucket foundations under vertical, horizontal, and moment loadings (Bransby and Randolph, 1998; Yun and Bransby, 2007; Hung and Kim, 2012; Hung and Kim, 2014).
If the bucket foundation is used as a wind turbine foundation, fatigue design is a very important issue. The effect of wind and wave cyclic loading to changes of soil properties has to be considered. However, the long-term cyclic response and the estimation of accurate accumulated rotation are the most important issues for design.
In this study, we performed a series of three-dimensional finite element analyses of bucket foundations installed in two different types of soils. An empirical formulation of stiffness degradation of soil is implemented into the analysis using a user subroutine. Using the stiffness degradation model the accumulated rotation and displacement of bucket foundation were calculated. Additionally, important factors affecting the deformation response under cyclic loading were assessed.

STIFFNESS DEGRADATION OF SOIL

Stiffness Degradation of Cohesionless Soil

The stiffness degradation model concept for cyclic loading effect is illustrated in Fig. 1. In a cyclic triaxial test, the degradation rate of secant stiffness can be presented by a reciprocal ratio of the plastic axial strain according to the Eq. 1, and the accumulation of plastic strains can be estimated from existing semi-empirical equation from the published literatures. In this study, the Huurman's formula (Huurman, 1996) is considered (Eq. 1~3).

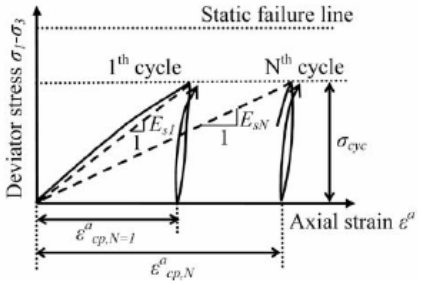

Figure 1. Concept of stiffness degradation model (Achmus, 2009)

$$\frac{E_{sN}}{E_{s1}} = \frac{\varepsilon^{a}_{cp,N=1}}{\varepsilon^{a}_{cp,N}} = N^{-b_1(X)^{b_2}} \quad (1)$$

where, E_{s1} = the secant stiffness after first cycle

E_{sN} = the secant stiffness after N^{th} cycle

$\varepsilon^{a}_{cp,N=1}$ = the plastic axial strain after first cycle

$\varepsilon^{a}_{cp,N}$ = the plastic axial strain after N^{th} cycle

N = the number of load cycles

X = the cyclic stress ratio

b_1 and b_2 = two material parameters

$$X = \frac{\sigma_{1,cyc}}{\sigma_{1,sf}} \quad (2)$$

where, $\sigma_{1,sf}$ = the major principal stress at static failure state

$\sigma_{1,cyc}$ = the major principal stress at cyclic failure state

In pile-soil system, the directions of the principal stresses are changed with the application of the load. To consider this issue, a characteristic cyclic stress ratio X_c is defined as follows. In Eq. 1, X is replaced X_c.

$$X_c = \frac{X^{(1)} - X^{(0)}}{1 - X^{(0)}} \quad (3)$$

where the index $^{(1)}$ means the cyclic stress ratio at loading state and the index $^{(0)}$ means at unloading state.

Stiffness Degradation of Cohesive Soil

The degradation of the secant shear modulus during cyclic loading can be measured by the degradation index δ. During a strain-controlled cyclic simple shear test, δ is defined as ratio between the shear stress after N cycles of constant shear strain amplitude and the shear stress in the first cycle (Eq. 4).

$$\delta = \frac{G_N}{G_1} = \frac{\left(\frac{\tau_N}{\gamma_c}\right)}{\left(\frac{\tau_1}{\gamma_c}\right)} = \frac{\tau_N}{\tau_1} = N^{-t} \quad (4)$$

where, G_1 = the secant shear modulus after first cycle

G_N = the secant shear modulus after N^{th} cycle

τ_1 = the shear stress after first cycle

τ_N = the shear stress after N^{th} cycle

γ_c = the constant shear strain amplitude

t = the degradation parameter

Fig. 2 shows the plot of t versus γ_c corresponding to the strain-controlled cyclic undrained simple shear test (CyUDSS) on the four highly plastic Venezuelan clays, and the low plasticity GAL clay (Vucetic et al., 1988). Based on the data points from previous tests, the two hyperbolic equations were independently fitted to two types of clay.

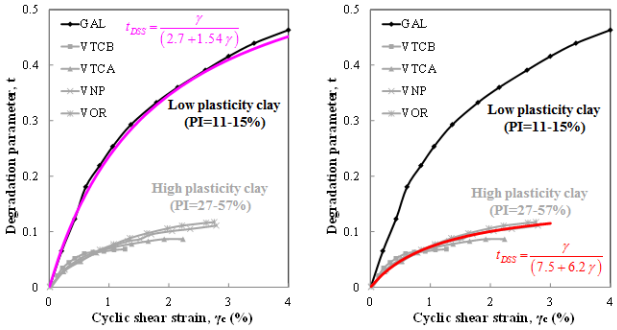

(a) Low plasticity clay (b) High plasticity clay

Figure 2. Variation of degradation parameter with γ_c and PI

Fig. 3 presents the plot of stiffness degradation δ versus N for high plasticity clay calculated from the proposed equation.

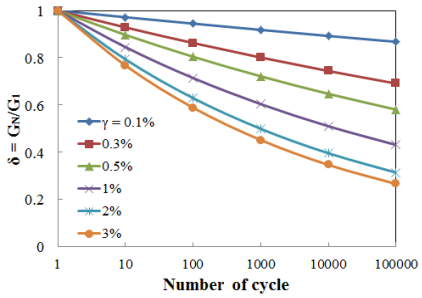

Figure 3. Degradation index versus number of cycles for high plasticity clay

FINITE ELEMENT MODEL

To investigate the long-term behavior of the bucket foundation installed in sand and clay layers, three-dimensional finite element analyses (FE) were performed using ABAQUS (Simulia, 2010). We did not simulate the penetration process of the bucket foundation, and assumed that it is "wished into" place.

Considering the symmetric condition, only half of the model was simulated to reduce the computation time (Fig. 4). The model dimensions were selected in order to avoid the influence of boundary on calculated response. The width of the lateral boundary from the center of the foundation was set to 10 D, whereas the depth of the soil profile from the tip of the foundation to the bottom of the computational domain was set to 7 L. The vertical and horizontal displacements were fixed at the bottom boundary and the horizontal displacement was constrained at the lateral boundaries and the symmetry plane. In this study, the diameter, length and thickness of bucket foundation model were kept constant (D = 17 m, L = 14 m, t = 0.5 m) for all analyses.

The eight nodded-linear brick element (C3D8) was used to model the soil and the structure. The size of the soil elements around the bucket

foundation was gradually reduced from the boundary to accurately model the abrupt change in stress and strain near the foundation. The accumulated lateral displacement and rotation were calculated using the load control method, which gradually increases the horizontal load (H) at the reference point (RP) located at a height e = M/H.

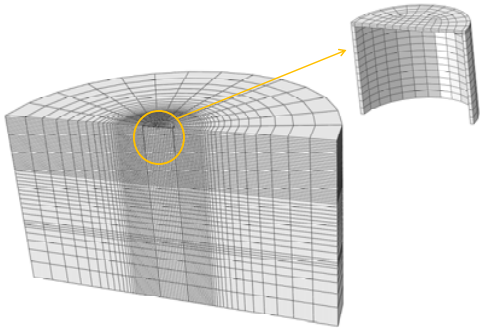

Figure 4. Computational model for the analysis

The linear elastic model was utilized for the bucket foundation. The Young's modulus E and Poisson's ratio v were 20,000 MPa and 0.2, respectively. The submerged unit weight of concrete was set to $\gamma' = 14$ kN/m^3.

The Tresca (Clay) and Mohr-Coulomb (Sand) models were used for the simulation of the soil behavior. The unit weight and shear strength s_u of clay were assumed to 8 kN/m^3 and 30 kPa. The Poisson's ratio was fixed to 0.49 to simulate the undrained behavior. The maximum shear modulus (G_{max}) of clay was estimated from following empirical equation (Wair et al., 2012), and the PI = 35 modulus reduction curve (G/G_{max}) from Vucetic and Dobry (1991) was used for simulation.

$$G_{\max} = \rho \cdot V_s^2 \tag{5}$$

$$V_s = 23 \cdot s_u^{0.475} \tag{6}$$

For stiffness degradation model, the effect of cyclic degradation on modulus reduction behavior of high plasticity clay is shown in Fig. 5.

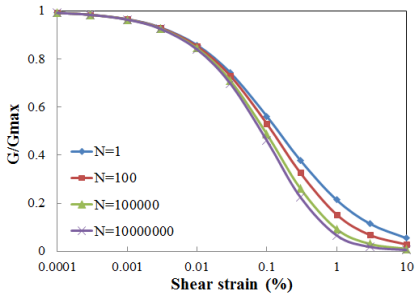

Figure 5. Input values of shear modulus degradation

The internal friction angle and dilatancy angle for dense sand were 40° and 10°, respectively. A small value of cohesion (c = 1 kPa) was used to enhance the stability of the analyses. The elastic modulus at first cycle (E_{s1}) and Poisson's ratio for sand were set to 30 MPa and 0.3. The effective unit weight of sand 9 kN/m^3 was applied. To account for the cyclic loading effect, the stiffness degradation concept (Eq. 1) was implemented in the numerical model. From cyclic triaxial test results in the literature, typical parameters (b_1, b_2) were shown for dense sand to be $b_1 = 0.2$, $b_2 = 5.76$ (Kuo, 2008).

For cohesive soil, the undrained shear strength was used for the interface strength, and the two-thirds of the internal friction angle was set to the interface friction angle ($\alpha = \tan(2/3\phi)$) in cohesionless soil.

RESULTS AND DISCUSSION

Cyclic Response of Bucket Foundation on Cohesionless Soil

Using the computational model described above, the parametric study was performed to identify the effect of load conditions. The selected design load conditions for comparison are listed in the following table.

Table 1. Load applied in numerical analysis

Load case No.	Vertical (kN)	Horizontal (kN)	Moment (kN·m)	Torsion (kN·m)
Ⅰ	77,339	10,883	213,457	488
Ⅱ	73,624	12,900	191,210	579
Ⅲ	61,174	6,043	187,969	3,708
Ⅳ	52,255	2,931	156,171	1,779
Ⅴ	85,293	1,562	38,279	459
Ⅵ	45,020	533	12,622	329

The relationship between accumulated rotation angle (θ) and the number of cycles (N) for the different combined cyclic load is shown in Fig. 6. In all cases, it can be seen that the first cycle causes the largest displacement than the following ones. And the accumulated rotation of bucket foundation increase with the number of cycles, but rate decreases.

In general, the accumulated angular rotation of the foundation is significantly affected by the magnitude of cyclic moment (Ⅰ, Ⅱ, Ⅲ, Ⅳ vs. Ⅴ, Ⅵ). Although the size of the moment is similar in case Ⅱ and Ⅲ, the permanent displacement is rapidly increased (case Ⅱ) when the large horizontal load is applied at lower height (e = M/H).

Comparing the results of load case Ⅲ and Ⅳ, the increasing rate of rotation angle is lager in the case Ⅳ. In case Ⅲ, the acting moment is larger, but the applied lager vertical load make improvement in ultimate moment capacity than the case Ⅳ.

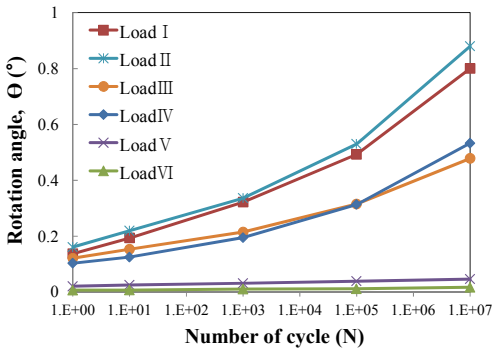

Figure 6. Accumulated angular rotation in relation to cycles

In Fig. 7, the changes of shear strain increment dependent on number of cycles are compared. The accumulation of plastic strain increases, as the stiffness of soil element decreases after a large number of cycles. The soil along the whole length of the skirt is influenced by stiffness degradation. The soil stiffness in the upper part and around the skirt tip on the passive side degrades significantly.

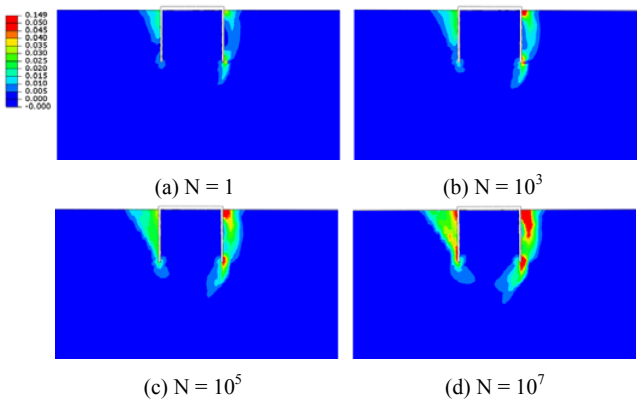

(a) N = 1 (b) N = 10^3

(c) N = 10^5 (d) N = 10^7

Figure 7. Variation of shear strain increment in soil dependent on the number of load cycles (Load case Ⅲ)

Cyclic Response of Bucket Foundation on Cohesive Soil

The vertical load due to the turbine weight 2,000 kN is considered for the analysis. And the moment can be achieved by applying the horizontal load 5,000 kN at a height 30 m above the lid of the foundation. The result shown the increase of the angular rotation at seabed level is given dependent on the number of load cycles in logarithmic scale. The angular rotation of bucket foundation is increased after 10,000,000 cycles by factor of 1.3.

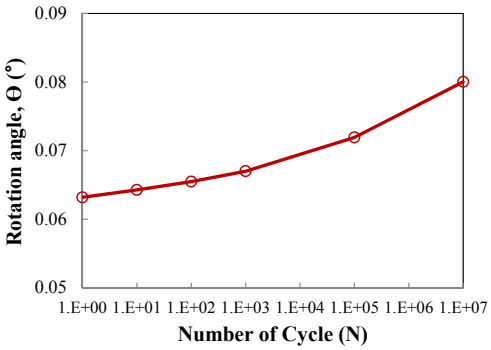

Figure 8. Accumulated angular rotation of the bucket foundation installed in cohesive soil

CONCLUSIONS

Bucket foundations can be used as foundations for offshore wind turbines. One of the critical issues in design of bucket foundations is the prediction of the cyclic response over the lifetime of the wind turbine. A stiffness degradation numerical model is implemented into a finite element analysis program to simulate the effect of cyclic lateral loading of foundations installed in sands and clays. The degradation model uses an empirical formulation which models the stiffness degradation observed in the results of the cyclic tests in laboratory.

As expected, the cyclically accumulated rotation of the foundation is significantly affected by the characteristics of applied load and the number of cycles. Further study would need a series of triaxial and simple shear tests to assess the parameters representing cyclic behavior of various soils. In addition, extensive numerical simulations are required to develop design charts for predicting the accumulated deformation of bucket foundation under long-term cyclic loading.

ACKNOWLEDGEMENTS

This work was supported by the project title 'Development of design basis and concrete technologies for offshore wind turbine support structures (20120093)' funded by the Ministry of Oceans and Fisheries, Republic of Korea.

REFERENCES

Achmus, M, Kuo, YS and Abdel-Rahman, K (2009). "Behavior of monopile foundations under cyclic lateral load," *Computers and Geotechnics*, 36(5), 725~735.

Bransby, MF, and Randolph, MF (1998). "Combined loading of skirted foundations," *Geotechnique*, 48(5), 637-655.

Hung, LC, and Kim, SR (2012) "Evaluation of vertical and horizontal bearing capacities of bucket foundations in clay," *Ocean Engineering*, 52, 75-82.

Hung, LC, and Kim, SR (2014). "Evaluation of undrained bearing capacities of bucket foundations under combined loads," *Marine Georesources & Geotechnology*, 32(1), 76-92.

Huurman, M (1996). "Development of traffic induced permanent strain in concrete block pavement," *Heron*, 41(1), 29-52.

Kuo, YS (2008). "On the behavior of large-diameter piles under cyclic lateral load," PhD thesis, Foundation Engineering and Waterpower Engineering, Leibniz University of Hannover.

Simulia (2010). *ABAQUS User's Manual*, Dassault Systemes Simulia Corp.

Vucetic, M, and Dobry, R (1988). "Degradation of marine clays under cyclic loading," *Journal of Geotechnical Engineering*, 114(2), 133~149.

Vucetic, M, and Dobry, R (1991). "Effect of soil plasticity on cyclic response," *Journal of Geotechnical Engineering*, 117(1), 89~107.

Wair, BR, DeJong, JT, and Shantz, T (2012). "Guidelines for estimation of shear wave velocity profiles," PEER, 1~68.

Yun, G, and Bransby, MF (2007). "The horizontal-moment capacity od embedded foundations in undrained soil," *Can. Geotech. J.*, 44(4), 409-427.

Zhu, B, Byrne, BW, and Houlsby, GT (2013). "Long-term lateral cyclic response of suction caisson foundations in sand," *Journal of Geotechnical and Geoenvironmental Engineering*, 139(1), 73~83.